

XMM–Newton observes flaring in the polar UZ For during a low state

Dirk Pandel^{*} and France A. Córdova

Department of Physics, University of California, Santa Barbara, CA 93106, USA

Accepted 2002 July 10. Received 2002 July 10; in original form 2002 May 21

ABSTRACT

During an *XMM–Newton* observation, the eclipsing polar UZ For was found in a peculiar state with an extremely low X-ray luminosity and occasional X-ray and ultraviolet (UV) flaring. For most of the observation, UZ For was only barely detected in X-rays and ~ 800 times fainter than during a high state previously observed with *ROSAT*. A transient event, which lasted ~ 900 s, was detected simultaneously by the X-ray instruments and, in the UV, by the Optical Monitor. The transient was likely caused by the impact of 10^{17} – 10^{18} g of gas on the main accretion region of the white dwarf. The X-ray spectrum of the transient is consistent with ~ 7 keV thermal bremsstrahlung from the shock-heated gas in the accretion column. A soft blackbody component resulting from reprocessing of X-rays in the white dwarf atmosphere is not seen. The increase in the UV flux during the transient was likely caused by cyclotron radiation from the shock-heated gas. Two more flaring events were detected by the Optical Monitor while the X-ray instruments were not operating. We conclude from our analysis that the unusual flaring behaviour during the low state of UZ For was caused by intermittent increases of the mass transfer rate owing to stellar activity on the secondary. In addition to the transient events, the Optical Monitor detected a roughly constant UV flux consistent with 11 000-K blackbody radiation from the photosphere of the white dwarf. We find a small orbital modulation of the UV flux caused by a large, heated pole cap around the main accretion region.

Key words: stars: activity – binaries: eclipsing – stars: individual: UZ For – stars: magnetic fields – novae, cataclysmic variables – X-rays: binaries.

1 INTRODUCTION

UZ For is an eclipsing member of the subclass of cataclysmic variables called AM Her binaries or polars. In these binaries, the strong magnetic field of the white dwarf primary causes it to rotate synchronously with the orbital motion. The magnetic field also prevents the formation of an accretion disc around the white dwarf. The accretion stream from the Roche lobe filling secondary is funnelled along the magnetic field lines and impacts the white dwarf near a magnetic pole. Slightly above the surface, the accretion stream forms a stand-off shock that heats the gas to temperatures in excess of 10^8 K. The shock-heated plasma then cools and settles on to the white dwarf while strongly emitting cyclotron radiation (IR to UV) and thermal bremsstrahlung (mostly X-rays). The photosphere below the shock is heated by reprocessing of X-rays and emits blackbody radiation visible at soft X-ray and UV energies. Many polars have been observed to decline in brightness by several magnitudes and remain in a faint state for days to years. The causes of these low states are not known, but, in the absence of an accretion disc, the large brightness variations must be due to changes in the mass transfer rate from

the companion star. A comprehensive review of polars is given in Warner (1995).

UZ For (EXO 033319-2554.2) was first detected as a serendipitous X-ray source with *EXOSAT* (Giommi et al. 1987; Osborne et al. 1988). Subsequent optical spectroscopy and polarimetry established UZ For as an eclipsing polar (Beuermann, Thomas & Schwöpe 1988; Berriman & Smith 1988). The 126.5-min orbital period is close to the lower edge of the 2–3 h ‘period gap’, a sparsely populated region in the orbital period distribution of cataclysmic variables. UZ For is a high inclination system ($i \approx 80^\circ$), and both accretion regions are eclipsed by the white dwarf for at least half of an orbital cycle. The optical spectrum of UZ For shows strong cyclotron emission lines which indicate magnetic fields of ~ 53 MG and ~ 48 MG for the two accretion poles (Rousseau et al. 1996). The best available estimates for the distance and the white dwarf mass are $d = 208 \pm 40$ pc and $M_{\text{WD}} \approx 0.6$ – $0.8 M_\odot$ (Ferrario et al. 1989; Bailey & Cropper 1991).

In this paper we present X-ray and UV data obtained with *XMM–Newton* while UZ For was in a state of unusually low and irregular accretion. We study the properties of an X-ray/UV flare and show that it was caused by accretion on to the white dwarf. We argue that the intermittent accretion rate increase was due to stellar activity on the companion star. Part of the *XMM–Newton* data has recently been

^{*}E-mail: dpandel@xmmoms.physics.ucsb.edu

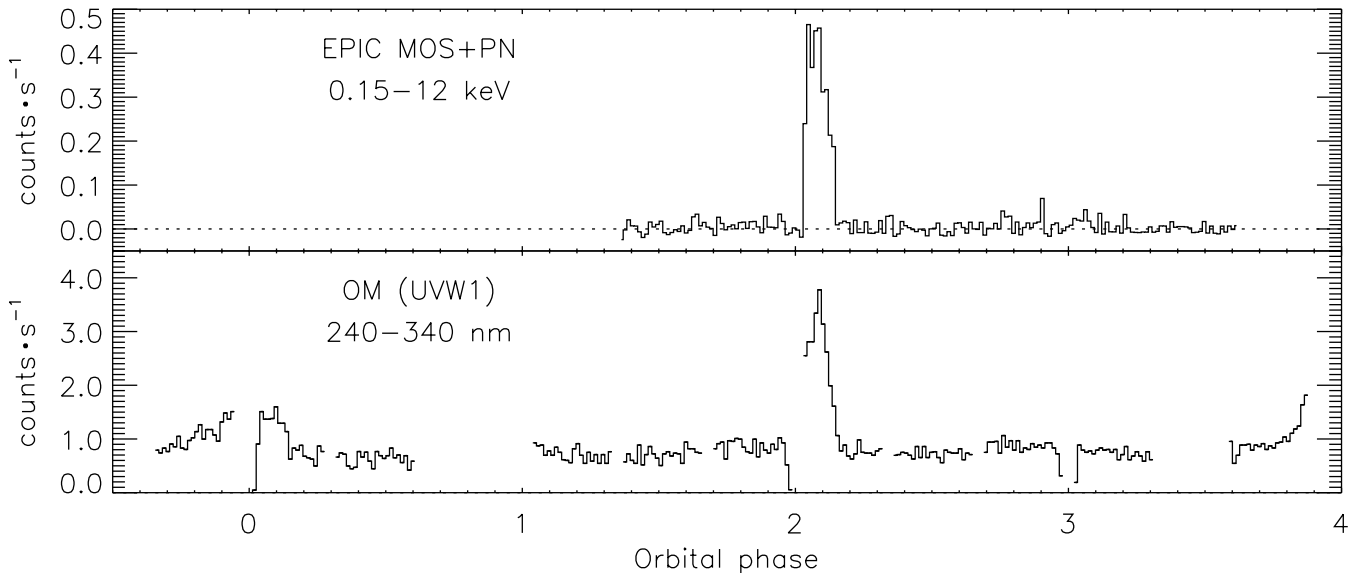


Figure 1. X-ray and UV light curves of UZ For obtained with *XMM-Newton* on 2001 January 14 (binning 100 s). Shown are the combined X-ray count rates of the three EPIC detectors (upper panel) and the UV count rate measured with the Optical Monitor using the UVW1 filter (lower panel). Orbital phase 0 is defined as the centre of the first eclipse as predicted by the ephemeris in Perryman et al. (2001).

published in Still & Mukai (2001). The goal of our paper is to utilize all available *XMM-Newton* data and present additional results not previously published. In particular, we find two more UV flares and clearly identify eclipses in the UV light curves. We show that the beginning of the X-ray/UV flare coincides with the eclipse egress of the main accretion region. This provides strong evidence that the flare was an accretion event on the white dwarf. We estimate the total accreted mass and show that it is consistent with the mass ejected by stellar flares on M dwarfs. We also detect a weak orbital modulation of the X-ray and UV fluxes and demonstrate that it is most likely due to emission from the main accretion region.

2 OBSERVATIONS AND ANALYSIS

UZ For was observed with *XMM-Newton* on 2001 January 14 as part of the performance verification of the mission. *XMM-Newton* (Jansen et al. 2001) carried out two separate observations, but during the first observation the EPIC cameras (Strüder et al. 2001; Turner et al. 2001) were used for calibration purposes, and only the Optical Monitor (Mason et al. 2001) was observing the source. During the second observation each of the three EPIC instruments performed one long exposure (16 ks for PN; 18 ks for MOS) with the thin blocking filters and the CCDs in large window mode. The Optical Monitor (OM) performed a total of 11 exposures of 2200 s duration each (three during the first and eight during the second observation). All OM exposures were done in fast mode (0.25-s timing resolution) and with the UVW1 filter (240–340 nm).

From the EPIC MOS and PN data we extracted good photon events (FLAG = 0) using a circular aperture centred on UZ For and with a 20-arcsec radius. Count rates quoted throughout the paper have been corrected for the 75 per cent enclosed energy fraction of this aperture. The background rate was estimated from a larger region on the same CCD as the source image. We included in our analysis events in the energy range 0.10–12 keV for the MOS and 0.15–12 keV for the PN. To maximize the signal-to-noise ratio, we used photon events with patterns 0–12. Only for the spectral analysis of the PN data did we select exclusively events with pattern 0. To

create X-ray light curves, we applied a barycentric correction to the photon arrival times and combined the events from all three EPIC instruments. For the extraction of UV light curves from the OM fast mode data, we used a circular aperture of 5.5-arcsec radius, which encloses 78 per cent of the detected source photons. Background subtracted UV and X-ray light curves of the available data are shown in Fig. 1. We defined as orbital phase zero the centre of the first eclipse as predicted by the most recent ephemeris (Perryman et al. 2001), which has an accumulated uncertainty of 4 s.

2.1 X-ray light curve

Except during a short flare, the X-ray flux from UZ For (Fig. 1) was at an extremely low level never before seen in this object. Even with the EPIC data integrated over the entire observation (excluding the flare), UZ For was detected only at a 4σ level. An improved 6σ detection could be achieved by limiting the integration to the orbital phase range 0.65–0.15. For these orbital phases, the main accretion region is on the side of the white dwarf facing us (Perryman et al. 2001). For orbital phases 0.15–0.65, for which the main accretion region is not visible, the integrated source count rate is consistent with zero at a 1σ level. It appears that the main accretion region was the source of the weak X-ray emission. We cannot rule out the possibility that the X-rays originated from the secondary region, which is visible for orbital phases 0.75–0.35. Yet one might expect that, as for other polars during low states, accretion was limited to the main region (e.g. Beuermann & Schwope 1989).

The combined EPIC MOS+PN count rate, averaged over the orbital phase range 0.65–0.15 (excluding the flare), is $0.009(2) \text{ s}^{-1}$ (0.15–12 keV). Ramsay et al. (1993) found, based on *ROSAT* observations, that the X-ray spectrum of UZ For in the high state is best described by an absorbed 28 eV blackbody below 0.5 keV plus a weak thermal bremsstrahlung tail visible at higher energies. Assuming this high-state spectrum, we would predict a *XMM-Newton* count rate of $\sim 7 \text{ s}^{-1}$, which is ~ 800 times higher than observed. The EPIC spectrum does not show any evidence of the blackbody component that was seen with *ROSAT*. However, the spectrum is in

good agreement with a thermal bremsstrahlung model. It is possible that, due to a lower temperature of the accretion spot, the blackbody component was shifted below 0.1 keV and not detectable by the EPIC instruments. This would require a blackbody temperature ≤ 15 eV, provided that the emitting area was the same as during the *ROSAT* observation. If we consider only the weak bremsstrahlung component found in the *ROSAT* spectrum, we would predict a *XMM–Newton* count rate of ~ 0.26 s $^{-1}$. This is still ~ 30 times higher than observed.

We estimated the total bremsstrahlung flux (excluding the flare) by fitting a single temperature thermal bremsstrahlung model to the EPIC spectra. With the temperature fixed at 10 keV, we obtained a bolometric bremsstrahlung flux $F_{\text{brems}} \approx 2 \times 10^{-14}$ erg cm $^{-2}$ s $^{-1}$. Of this flux, 80 per cent was inside the 0.10–12 keV energy range and directly detected by *XMM–Newton*. For a distance $d = 200$ pc, the corresponding bolometric luminosity is $L_{\text{brems}} \approx 7 \times 10^{28}$ erg s $^{-1}$. Here we used a geometric factor of 3.1π , which takes into account the scattering of X-rays off the surface of the white dwarf (King & Watson 1987). Assuming that all of the accretion energy was emitted in the bremsstrahlung component, we can estimate the accretion rate \dot{M} using $L_{\text{brems}} \approx GM_{\text{WD}}\dot{M}/R_{\text{WD}}$. For a white dwarf with a mass $M_{\text{WD}} = 0.7 M_{\odot}$ and a radius $R_{\text{WD}} = 8 \times 10^8$ cm, we find $\dot{M} \approx 6 \times 10^{11}$ g s $^{-1}$. This is likely an underestimate, since at such a low accretion rate most of the energy would be emitted as cyclotron radiation. For the parameters of UZ For, the calculations by Woelk & Beuermann (1996, their fig. 9) predict that cyclotron cooling dominates at specific accretion rates $\dot{m} < 10$ g cm $^{-2}$ s $^{-1}$. Therefore, if most of the energy were radiated as bremsstrahlung, accretion would have to occur in an unreasonably small region with $f \leq 10^{-8}$ (f is the area as a fraction of the surface area of the white dwarf). For a more typical spot size of $f = 5 \times 10^{-4}$ (Rousseau et al. 1996), we estimate from fig. 9 in Woelk & Beuermann (1996) that the cyclotron luminosity is $\sim 10^2 \times L_{\text{brems}}$. The corresponding accretion rate of 10^{13} – 10^{14} g s $^{-1}$ is comparable to that determined by Rousseau et al. (1996) for the low state of UZ For.

As shown in Fig. 1, a short flare was detected simultaneously by the X-ray instruments and the Optical Monitor. The flare (Fig. 2), which lasted ~ 900 s, increased the X-ray flux by a factor of ~ 30 . This is comparable to the flux that we estimated for the bremsstrahlung component during the high state (see above). The beginning of the flare at BJD(TT) 245 1924.244 01(2) coincides to within a few seconds with the eclipse egress of UZ For (see also Section 2.2). This is strong evidence that the flare emission originates from the white dwarf in UZ For. We will discuss the spectral properties of the flare in Section 2.3.

2.2 UV light curve

During most of the observation, the UV flux detected with the Optical Monitor was at a roughly constant level (Fig. 1). Besides the flare that was also detected with the EPIC instruments, two more flaring events are seen near orbital phases 0 and 4. Unfortunately, no X-ray data is available for these time periods. It should be noted that the flaring activity is only seen inside the orbital phase range 0.65–0.15 for which the main accretion region is visible. This is a further indication that the flaring is caused by accretion on to the main pole.

We were able to identify the ingress and egress for several eclipses of the white dwarf by the companion star (see Fig. 1 near integer orbital phases). Coincidentally, each of the eclipses overlapped, at least partially, with a gap in the OM data. We did not detect any UV emission during the eclipses, even after integrating all 530 s

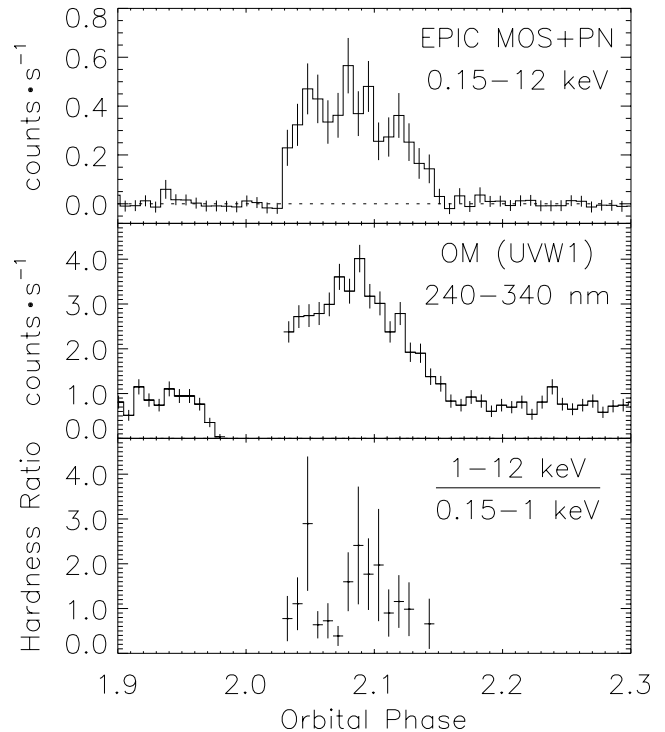


Figure 2. X-ray light curve, UV light curve, and X-ray hardness ratio of the flare near orbital phase 2 (binning 60 s).

of available eclipse data. This non-detection corresponds to an upper count rate limit of 0.05 s $^{-1}$ (3σ) or a flux limit of 2.5×10^{-17} erg cm $^{-2}$ s $^{-1}$ Å $^{-1}$ at 270 nm. Besides the accretion stream, the only potential source of emission during eclipse is the M-dwarf companion. Consistent with our limit, the models of Houdebine et al. (1996) predict a flux of 10^{-18} – 10^{-16} erg cm $^{-2}$ s $^{-1}$ Å $^{-1}$ for the companion in UZ For. Because of the fast rise and decline during eclipse, the white dwarf is probably the sole source of the UV emission. Due to the low accretion rate, a significant contribution from the accretion stream is unlikely.

The roughly constant UV count rate of 0.75 s $^{-1}$ that is seen during most of the observation is probably thermal emission from the photosphere of the white dwarf. The corresponding flux of 3.8×10^{-16} erg cm $^{-2}$ s $^{-1}$ Å $^{-1}$ at 270 nm is consistent with blackbody radiation from a 11 000-K white dwarf ($R_{\text{WD}} = 8 \times 10^8$ cm, $d = 200$ pc). The temperature is in agreement with that measured by Bailey & Cropper (1991). We find that the UV light curve (excluding the flares) has a sinusoidal orbital modulation of ~ 30 per cent (Fig. 3). The peak of the modulation is seen at orbital phase 0.88(2). Based on the spot longitudes determined by Perryman et al. (2001), we predict that emission from the main accretion region peaks at phase ~ 0.88 , while that from the secondary region peaks at ~ 0.03 . This strongly suggests that the modulated flux is thermal radiation from the heated photosphere near the main accretion spot. Another possible origin of the modulation is cyclotron radiation from the accretion column. Then, however, one would expect to see a double-peaked light curve with peaks near orbital phases 0.15 and 0.65. Although cyclotron radiation probably dominates the energy output from the accretion column, only a small fraction of it (< 1 per cent) is emitted in the UV. Assuming that the modulation is due to blackbody radiation from the main accretion region, we find that the flux excess of 1.2×10^{-16} erg cm $^{-2}$ s $^{-1}$ Å $^{-1}$ at 270 nm is equivalent to a luminosity of 4.2×10^{26} erg s $^{-1}$ Å $^{-1}$ ($d = 200$ pc). Because the accretion region

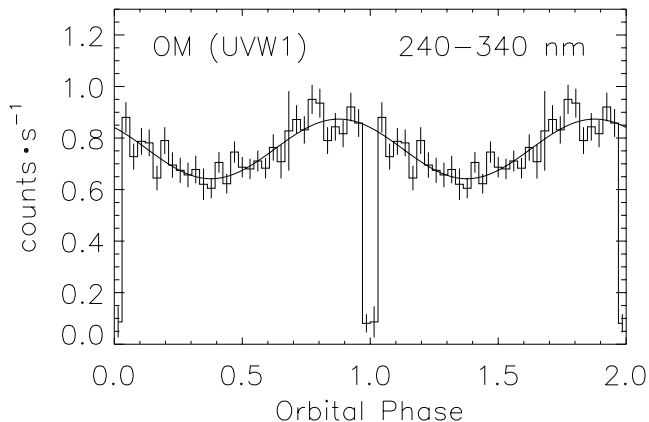


Figure 3. UV light curve folded on the orbital period after exclusion of the three flares shown in Fig. 1 (binning 230 s). Also shown is the best fit of a sine function to the orbital modulation (amplitude 30 per cent, maximum at phase 0.88).

is optically thick and inclined with respect to the line of sight, we applied a geometric correction of $\pi \cos^{-1}(\delta - i) \approx 9.2$ (inclination $i \approx 80^\circ$, colatitude $\delta \approx 150^\circ$; from Perryman et al. 2001). As discussed in Section 2.1, we could not identify a blackbody component in the X-ray spectrum. Using this non-detection, we can place an upper limit on the blackbody temperature. Depending on the hydrogen column density, which is in the range $0.25\text{--}1.3 \times 10^{20} \text{ cm}^{-2}$ (Osborne et al. 1988), we find a limit of $7\text{--}11 \text{ eV}$ (80 000–130 000 K). We can also constrain the bolometric blackbody luminosity $L_{\text{bb}} \leq 1 \times 10^{32} \text{ erg s}^{-1}$ and the size of the emitting region $f \geq 0.001$. The limit on L_{bb} is fairly high, $\sim 10^3$ times higher than the bolometric bremsstrahlung luminosity L_{brems} . It is therefore likely that the actual temperature of the emitting region is significantly lower than the upper limit. The lowest possible blackbody luminosity consistent with the observed UV flux is $1.5 \times 10^{30} \text{ erg s}^{-1}$ (for $kT_{\text{bb}} = 1.1 \text{ eV}$). This is still ~ 20 times higher than L_{brems} . A large ratio of blackbody to bremsstrahlung luminosity is found in many polars, typically at high accretion rates. This ‘soft excess’ is commonly explained by blobs in the accretion stream that penetrate deep into the photosphere (Frank, King & Lasota 1988). Blackbody radiation from this process is only emitted in the fairly small accretion region. In UZ For, however, the UV flux is varying sinusoidally even when the main accretion spot is not visible (phases 0.15–0.65). This is only possible if the emitting region is significantly larger than the accretion spot and comparable in size to the white dwarf. Apparently, we are seeing a large heated region of the photosphere of the white dwarf around the main accretion spot. For a covering fraction $f = 0.5$, this region has to be, on average, $\sim 1000 \text{ K}$ hotter than the other half of the surface of the white dwarf. Since L_{bb} is much larger than L_{brems} , reprocessing of X-rays is unlikely to be responsible for the heating of this region. However, the cyclotron luminosity is expected to be much larger than L_{brems} and might provide sufficient energy (see Section 2.1). It is also possible that we are seeing the afterglow from an earlier state of high accretion rate, since the time-scale for cooling of a heated pole cap is on the order of tens of days (Gänsicke 1997).

We determined the times of mid-ingress and mid-egress by fitting the profile expected for a circular emission region to the eclipses in the UV light curve (Fig. 1). Except for the egress near phase 2, we could not obtain useful constraints for the duration of ingress or egress. We therefore assumed a fixed value of 40 s, which is the time it takes to eclipse the entire white dwarf (Bailey & Cropper 1991).

Table 1. Fitted times/phases of mid-ingress and mid-egress of the eclipses in the UV light curve. The times/phases are relative to the eclipse centres as predicted by the ephemeris in Perryman et al. (2001), which has an accumulated uncertainty of 4 s. In all but one case, the ingress/egress duration could not be fitted and was fixed at 40 s. Uncertainties are given at a 1σ confidence level.

		Time	Phase	Duration
Ingress	Phase 2	$-225 \pm 4 \text{ s}$	$-0.0296(5)$	40 s
	Phase 3	$-220 \pm 5 \text{ s}$	$-0.0290(7)$	40 s
Egress	Phase 0	$+220 \pm 4 \text{ s}$	$+0.0290(7)$	40 s
	Phase 2	$+233 \pm 2 \text{ s}$	$+0.0307(3)$	$3 \pm 3 \text{ s}$
	Phase 3	$+233 \pm 5 \text{ s}$	$+0.0307(7)$	40 s

Although not apparent in the UV light curve (Fig. 2), the egress near phase 2, just before the flare, can be clearly identified. About 10 s after the beginning of the new OM exposure, the count rate increased quickly from 0 to $\sim 3 \text{ s}^{-1}$. This fast rise coincides with the beginning of the flare in the X-ray light curve. The egress duration of $3 \pm 3 \text{ s}$ in the UV is similar to that measured in the optical for the main accretion region ($\sim 2 \text{ s}$; Bailey & Cropper 1991). Table 1 shows the fitted times/phases of mid-ingress and mid-egress relative to the eclipse centres. Using high time-resolution optical light curves of the eclipse, Perryman et al. (2001) resolved two distinct accretion regions. They found that the egress of the main region (Spot 1) occurs at phase 0.032, while that of the secondary region (Spot 2) occurs at phase 0.027. The beginning of the flare at phase 0.0307 is in good agreement with the egress of spot 1. This result strongly suggests that the flare was caused by accretion on to the main region and that the onset of the flare was hidden from us by the eclipse. In agreement with this interpretation, the end of the flare (Fig. 2) is seen at the same orbital phase of 0.15 at which the main accretion region disappears behind the white dwarf.

2.3 Flare spectrum

As shown in the previous sections, the X-ray/UV flare near orbital phase 2 was most likely caused by a significant increase in the rate of accretion on to the white dwarf. According to the picture of the standard accretion column, the X-ray spectrum of the flare should therefore consist of two spectral components, a bremsstrahlung component from the shock-heated gas and a blackbody component due to reprocessing of hard X-rays in the atmosphere of the white dwarf. We find that the flare spectrum (Fig. 4) is consistent with a pure bremsstrahlung model but does not show statistically significant evidence for a blackbody component. In particular, we do not find the 28-eV blackbody that dominated the *ROSAT* spectrum during the high state (Ramsay et al. 1993), despite the similar bremsstrahlung fluxes during both observations (Section 3.1). It is plausible that, during the *XMM-Newton* observation, accretion occurred over a larger area, leading to a blackbody temperature too low for a detection by the EPIC instruments. A lower blackbody temperature is also expected in the absence of blobs in the accretion stream. Such blobs were likely present during the *ROSAT* observation, as Ramsay et al. (1993) found a large soft X-ray excess. Dense blobs impacting the white dwarf are thought to heat small areas of the photosphere to higher temperatures than the reprocessing of hard X-rays (Hameury & King 1988). Without blobs in the accretion stream, the blackbody temperature would be much lower than the 28 eV found for the high state. As discussed later, a blackbody component with a temperature below $\sim 12 \text{ eV}$ was possibly detected in the UV. The hardness ratio in Fig. 2 indicates some spectral variability, which is likely due to irregularities in the accretion stream.

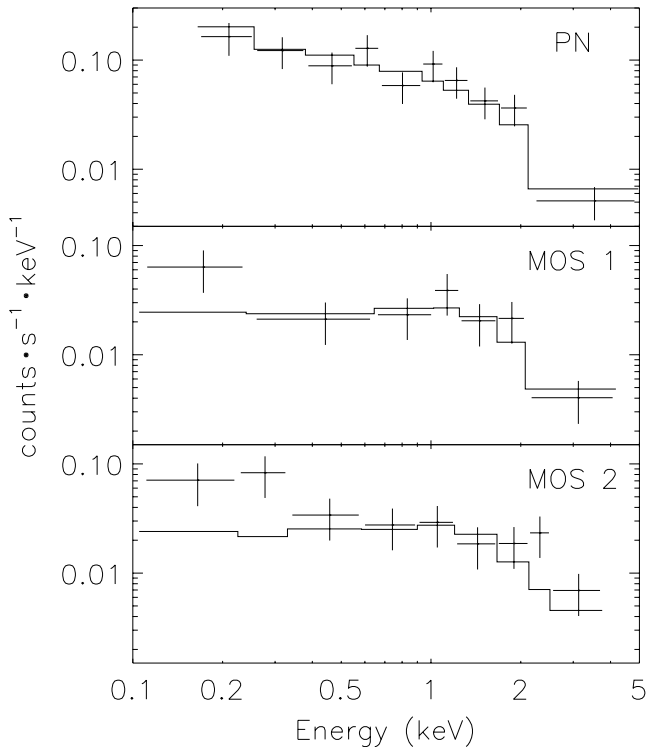


Figure 4. Average X-ray spectrum of the flare near orbital phase 2 shown separately for the three EPIC detectors. The solid lines represent the best fit of an absorbed single-temperature bremsstrahlung model with $kT_{\text{brems}} = 6.6$ keV and $N_{\text{H}} = 0.5 \times 10^{20}$ cm $^{-2}$.

The X-ray spectrum of the flare is well fit by a single-temperature thermal bremsstrahlung model ($\chi_{\text{red}}^2 \approx 1$). We included interstellar absorption in the model fit but could not obtain useful constraints for the hydrogen column density N_{H} . An upper limit of 1×10^{20} cm $^{-2}$ follows from the total galactic hydrogen column density in the direction of UZ For (Stark et al. 1992). Osborne et al. (1988) constrained N_{H} to the range 2.5×10^{19} – 1.3×10^{20} cm $^{-2}$. Table 2 shows the fitted temperature and unabsorbed bolometric flux of the bremsstrahlung model for various fixed column densities. The temperature of ~ 7 keV is typical for bremsstrahlung from the accretion column and similar to that found by Rousseau et al. (1996) from the cyclotron spectrum. For a distance $d = 200$ pc we obtain an unabsorbed bolometric luminosity $L_{\text{brems}} \approx 2.4 \times 10^{30}$ erg s $^{-1}$ (we used a geometric factor of 3.1π as in Section 2.1). This luminosity corresponds to a mass accretion rate $\dot{M} \approx 2 \times 10^{13}$ g s $^{-1}$ ($M_{\text{WD}} = 0.7 M_{\odot}$, $R_{\text{WD}} = 8 \times 10^8$ cm). A constant temperature model likely oversimplifies the flare spectrum, which shows considerable temporal variability (see hardness ratio in Fig. 2). However, the low signal-to-noise ratio of the data did not allow us to obtain use-

Table 2. Temperature and unabsorbed bolometric flux obtained from a fit of a bremsstrahlung model to the EPIC spectra of the flare. Results are shown for various fixed column densities N_{H} . The uncertainties of kT_{brems} are given at a 1σ confidence level.

N_{H} [cm $^{-2}$]	kT_{brems} [keV]	F_{brems} [erg cm $^{-2}$ s $^{-1}$]
0.2×10^{20}	$7.5^{+6.8}_{-2.7}$	6.8×10^{-13}
0.5×10^{20}	$6.6^{+5.1}_{-2.2}$	6.5×10^{-13}
1.0×10^{20}	$5.7^{+3.8}_{-1.8}$	6.0×10^{-13}

ful estimates for the temperature variations during the flare. Since ~ 80 per cent of the flux in the constant temperature model is inside the 0.15–12 keV energy range and directly detected by XMM–Newton, a constant temperature fit should provide a good estimate for the bolometric bremsstrahlung flux, despite the spectral variability.

In the Optical Monitor, the flare (Fig. 2) caused an average count rate increase of ~ 2 s $^{-1}$, which corresponds to a flux of 1×10^{-15} erg cm $^{-2}$ s $^{-1}$ Å $^{-1}$ at 270 nm or an integrated flux in the 240–340 nm band of the UVW1 filter of $F_{\text{UVW1}} \approx 1 \times 10^{-12}$ erg cm $^{-2}$ s $^{-1}$. The latter value is comparable to the bolometric bremsstrahlung flux F_{brems} . The likely origin of the UV emission is either cyclotron radiation from the post-shock region or blackbody radiation from the photosphere below the shock (or a combination of the two). The XMM–Newton data do not allow us to distinguish between the two possibilities.

UZ For is known to be a strong emitter of cyclotron radiation (Schwope, Beuermann & Thomas 1990). Past observations of the cyclotron spectrum covered only optical wavelengths, but model calculations by Rousseau et al. (1996) suggest that cyclotron emission lines may be present in the near UV. If the Optical Monitor did indeed detect cyclotron radiation, only a small fraction of the total cyclotron flux was actually seen. Using the results by Woelk & Beuermann (1996) in a similar way as in Section 2.1, we estimate that the cyclotron luminosity was 10^1 – 10^2 times higher than L_{brems} . This luminosity corresponds to an accretion rate of 10^{14} – 10^{15} g s $^{-1}$ or a total accreted mass of 10^{17} – 10^{18} g for the duration of the flare.

The accretion region is heated by reprocessing of X-rays from the post-shock region or by blobs in the accretion stream that penetrate several scale heights into the atmosphere. This gives rise to blackbody radiation visible at X-ray and UV energies (Warner 1995). Assuming that all of the UV flare emission is due to this blackbody, we estimate a luminosity of 4×10^{27} erg s $^{-1}$ Å $^{-1}$ at 270 nm ($d = 200$ pc). As in Section 2.2 we used a geometric factor of 9.2. Since the blackbody component is not visible in the X-ray spectrum, we can place an upper limit of 7–12 eV on its temperature. The uncertainty derives mostly from the not well known hydrogen column density $N_{\text{H}} = 0.25$ – 1.3×10^{20} cm $^{-2}$ (Osborne et al. 1988). (The EPIC MOS spectra in Fig. 4 show a small excess over the bremsstrahlung model at low energies. This might be considered marginal evidence for the blackbody component but could also be due to calibration uncertainties below 0.2 keV.) The limit on the blackbody temperature also puts constraints on the effective emitting area $f_{\text{eff}} \geq 0.01$ and the blackbody luminosity $L_{\text{bb}} \leq 0.3$ – 1.5×10^{33} erg s $^{-1}$. The actual luminosity is likely close to this limit, since a significantly smaller L_{bb} would require an unreasonably large emitting area $f \gg 0.01$. In particular, it is not possible that $L_{\text{bb}} \approx L_{\text{brems}}$, which rules out reprocessing of X-rays as a major contributor to the UV flux. The large ratio $L_{\text{bb}}/L_{\text{brems}} \sim 10^2$ could be due to blobs in the accretion stream (Frank et al. 1988). Then, however, one might expect f_{eff} to be smaller than our limit of 0.01. An effective emitting area $f_{\text{eff}} < 10^{-4}$ is required for the 28 eV blackbody found by Ramsay et al. (1993) in the ROSAT spectrum. (As discussed in Hameury & King (1988), f_{eff} can be substantially smaller than the size of the accretion region.) Considering these difficulties, it seems unlikely that a large fraction of the UV flare emission is blackbody radiation from the accretion region.

3 DISCUSSION

UZ For was found in a peculiar state that could have been classified as a regular low state if XMM–Newton had not detected several

X-rays/UV flares. Whereas flaring is common during the high state and probably due to dense blobs in the accretion stream (Hameury & King 1988), flaring during a low state has only been reported for two other polars. *EUVE* detected two transient events, each lasting ~ 1 h, during a low state of QS Tel (Warren et al. 1993). Three possible explanations for the transients were suggested: magnetic flares on the secondary; dense filaments in the accretion stream impacting the white dwarf; intermittently enhanced mass transfer from the secondary caused by magnetic flares or coronal mass ejections. In AM Her, Shakhovskoy et al. (1993) observed an optical transient that lasted ~ 20 min and increased the brightness by 2 mag. The properties of the transient (exponential decay, blue colour, no polarization) strongly suggest emission from a stellar flare on the companion star. Also in AM Her, Bonnet-Bidaud et al. (2000) observed several smaller transients (~ 0.5 mag) that were red in colour and circularly polarized. These transients were likely caused by irregular accretion on to the white dwarf (e.g. by filaments in the accretion stream).

Our analysis of the *XMM-Newton* data clearly shows that the flaring in UZ For was caused by accretion on to the white dwarf. This rules out magnetic flares on the secondary as the source of the X-ray and UV emission. It is also unlikely that dense filaments in an otherwise constant accretion stream caused the large increase in X-ray luminosity. The observed bremsstrahlung spectrum and the absence of a blackbody component indicate that the shock was not buried in the photosphere, as is expected for dense filaments impacting the white dwarf. The most likely explanation for the flaring in UZ For is an intermittent increase in the mass transfer rate from the companion star.

The causes of high and low states in polars are still poorly understood. Unlike other CVs, polars do not have an accretion disc, so that changes in the rate of accretion on to the white dwarf must be due to variations of the mass flow rate through the L1-point. Variations in the size of the secondary or of the Roche lobe cannot be the cause of low states, as those changes occur on time-scales of 10^4 – 10^5 yr (King et al. 1995; Ritter 1988). However, Howell et al. (2000) showed that for secondaries in short-period CVs the critical Roche surface is well above the photosphere, so that mass flow rates through the L1-point are controlled by the chromosphere. Changes in an active chromosphere can occur on time-scale short enough to explain the low states in polars. Alternatively, it has been suggested that star spots may appear at the L1-point and greatly reduce the mass transfer rate (Livio & Pringle 1994; King & Cannizzo 1998; Hessman, Gänsicke & Mattei 2000). However, Howell et al. (2000) point out that, for short-period CVs, star spots exist well below the critical Roche surface, and the magnetic activity near the spots might actually increase the accretion rate. In both scenarios, it is possible that coronal mass ejections or solar flares near the L1-point intermittently increase the mass transfer rate, thus causing accretion events as those seen in UZ For.

Little is known about the level of stellar activity in CV secondaries. But because of their rapid rotation, which is synchronized with the binary orbital motion, an active atmosphere can be expected. A number of observations suggest that star spots and magnetic flares do exist on CV secondaries (e.g. Howell et al. 2000; Webb, Naylor & Jeffries 2002; Shakhovskoy et al. 1993). We showed that the X-ray transient in UZ For was caused by accretion of 10^{17} – 10^{18} g of gas on to the white dwarf. It is not unreasonable that this much mass was ejected by a flare on the dM4.5 companion star. From observations of stellar flares on nearby M dwarfs, Pallavicini, Tagliaferri & Stella (1990) estimated a density range of $\leq 10^{12}$ – 10^{13} cm $^{-3}$ and a volume range of $\geq 10^{27}$ – 10^{29} cm 3 , corresponding

to flare masses of 10^{15} – 10^{18} g. For the largest flares, peak X-ray luminosities up to $\sim 10^{30}$ erg s $^{-1}$ (0.05–2 keV) were measured. A flare with such a high luminosity would have been detected by *XMM-Newton* with an EPIC count rate of ~ 0.2 s $^{-1}$ over $\sim 10^3$ s. Since no emission from the companion star was seen, the X-ray luminosity of any stellar flare must have been below $\sim 10^{29}$ erg s $^{-1}$. Coronal X-ray emission other than that from large stellar flares is unlikely to be detectable, even with the data integrated over the entire observation. For the most active stars of type dM5 or later, Fleming et al. (1993) measured average X-ray luminosities up to 10^{28} erg s $^{-1}$ (0.1–2.4 keV). The corresponding EPIC count rate of ~ 0.002 s $^{-1}$ is slightly below the detection threshold for the UZ For observation. We conclude that, despite the absence of X-ray emission from the companion star, accretion of gas ejected by stellar flares is a viable explanation for the transient events observed in UZ For.

4 CONCLUSION

During the *XMM-Newton* observation, UZ For was found in an extremely low accretion state with an X-ray luminosity ~ 800 times fainter than during a high state previously observed with *ROSAT*. Occasional X-ray and UV flaring was detected by the X-ray instruments and the Optical Monitor. The largest flare lasted ~ 900 s and increased the X-ray flux by a factor of ~ 30 . We found that the beginning of this flare coincided to within a few seconds with the eclipse egress of the main accretion region. This provides strong evidence that the flaring was caused by accretion on to the white dwarf. The X-ray spectrum of the flare is consistent with ~ 7 keV thermal bremsstrahlung from the accretion column. A blackbody component, as seen with *ROSAT* during the high state, was not found. It is plausible that, because of a larger accretion region or the absence of blobs in the accretion stream, the blackbody temperature was too low for a detection by the X-ray instruments. The increase in the UV flux seen during the flare was probably caused by cyclotron radiation from the accretion column. A significant contribution of blackbody radiation to the UV flare emission is unlikely as this would require a very large soft excess. Under the assumption that all accretion energy is emitted as bremsstrahlung, we estimate an accretion rate of 2×10^{13} g s $^{-1}$ during the flare. However, since at this low rate most of the energy is emitted as cyclotron radiation, the actual accretion rate was probably 10^1 – 10^2 times higher. We therefore estimate that during the flare a total of 10^{17} – 10^{18} g of gas was accreted on to the white dwarf. The likely cause of the flaring observed in UZ For is stellar activity on the companion star that intermittently increased the mass transfer rate near the L1-point. The mass that was accreted on to the white dwarf during the large transient is consistent with the mass ejected by a stellar flare.

Before and after the X-ray transient, extremely weak X-ray emission, possibly due to the regular low-state accretion on to the main region, was detected. The observed X-ray luminosity corresponds to an accretion rate of 6×10^{11} g s $^{-1}$. Since cyclotron radiation dominated the energy output, the actual accretion rate was probably 10^{13} – 10^{14} g s $^{-1}$, which is similar to the rates estimated for previous low states. In addition to the flare emission, we detect a roughly constant UV flux consistent with blackbody radiation from a 11000-K white dwarf. A small orbital modulation of the UV flux indicates the presence of a large, heated pole cap around the main accretion region.

Flaring during a low state has only been observed for a few polars. This may be due to insufficient monitoring of polars in low states. Yet low-state observations are essential since, during high

and intermediate states, flaring caused by stellar activity on the companion star is likely overlooked and mistakenly attributed to accretion stream instabilities. Future low-state observations will reveal how common flaring due to stellar activity is among polars. An interesting question that might also be answered is, whether flaring occurs preferentially at the beginning or end of low states. Monitoring of irregular accretion in low-state polars may provide a new way to study stellar flares or other types of mass ejections that are too faint to be observed directly.

ACKNOWLEDGMENTS

This work is based on observations obtained with *XMM–Newton*, an ESA science mission with instruments and contributions directly funded by ESA Member States and the USA (NASA). The authors acknowledge support from NASA grant NAG5-7714.

REFERENCES

- Bailey J., Cropper M., 1991, *MNRAS*, 253, 27
 Berriman G., Smith P. S., 1988, *ApJ*, 329, L97
 Beuermann K., Schwobe A. D., 1989, *A&A*, 223, 179
 Beuermann K., Thomas H.-C., Schwobe A., 1988, *A&A*, 195, L15
 Bonnet-Bidaud J. M. et al., 2000, *A&A*, 354, 1003
 Ferrario L., Wickramasinghe D. T., Bailey J., Tuohy I. R., Hough J. H., 1989, *ApJ*, 337, 832
 Fleming T. A., Giampapa M. S., Schmitt J. H. M. M., Bookbinder J. A., 1993, *ApJ*, 410, 387
 Frank J., King A. R., Lasota J.-P., 1988, *A&A*, 193, 113
 Gänsicke B. T., 1997, PhD Thesis, George-August Uni., Göttingen
 Giommi P., Angelini L., Osborne J., Stella L., Tagliaferri G., Beuermann K., Thomas H.-C., 1987, *IAU Circ.*, 4486, 1
 Hameury J. M., King A. R., 1988, *MNRAS*, 235, 433
 Hessman F. V., Gänsicke B. T., Mattei J. A., 2000, *A&A*, 361, 952
 Houdebine E. R., Mathioudakis M., Doyle J. G., Foing B. H., 1996, *A&A*, 305, 209
 Howell S. B., Ciardi D. R., Dhillon V. S., Skidmore W., 2000, *ApJ*, 530, 904
 Jansen F. et al., 2001, *A&A*, 365, L1
 King A. R., Cannizzo J. K., 1998, *ApJ*, 499, 348
 King A. R., Watson M. G., 1987, *MNRAS*, 227, 205
 King A. R., Frank J., Kolb U., Ritter H., 1995, *ApJ*, 444, L37
 Livio M., Pringle J. E., 1994, *ApJ*, 427, 956
 Mason K. O. et al., 2001, *A&A*, 365, L36
 Osborne J. P., Giommi P., Angelini L., Tagliaferri G., Stella L., 1988, *ApJ*, 328, L45
 Pallavicini R., Tagliaferri G., Stella L., 1990, *A&A*, 228, 403
 Perryman M. A. C., Cropper M., Ramsay G., Favata F., Peacock A., Rando N., Reynolds A., 2001, *MNRAS*, 324, 899
 Ramsay G., Rosen S. R., Mason K. O., Cropper M. S., Watson M. G., 1993, *MNRAS*, 262, 993
 Ritter H., 1988, *A&A*, 202, 93
 Rousseau T., Fischer A., Beuermann K., Woelk U., 1996, *A&A*, 310, 526
 Schwobe A. D., Beuermann K., Thomas H.-C., 1990, *A&A*, 230, 120
 Shakhovskoy N. M., Alexeev I. Y., Andronov I. L., Kolesnikov S. V., 1993, *Ann. Israel Phys. Soc.*, 10, 237
 Stark A. A., Gammie C. F., Wilson R. W., Bally J., Linke R. A., Heiles C., Hurwitz M., 1992, *ApJS*, 79, 77
 Still M., Mukai K., 2001, *ApJ*, 562, L71
 Strüder L. et al., 2001, *A&A*, 365, L18
 Turner M. J. L. et al., 2001, *A&A*, 365, L27
 Warner B., 1995, *Cambridge Astrophysics Series*, Cataclysmic variable stars. Cambridge Univ. Press, Cambridge
 Warren J. K., Vallergera J. V., Mauche C. W., Mukai K., Siegmund O. H. W., 1993, *ApJ*, 414, L69
 Webb N. A., Naylor T., Jeffries R. D., 2002, *ApJ*, 568, L45
 Woelk U., Beuermann K., 1996, *A&A*, 306, 232

This paper has been typeset from a $\text{\TeX}/\text{\LaTeX}$ file prepared by the author.